

1
2
3
4
5
6
7
8
9
10
11
12
13
14
15
16
17
18
19
20
21

**Ammonia impacts methane oxidation and methanotrophic community in
freshwater sediment**

Yuyin Yang¹, Jianfei Chen¹, Shuguang Xie^{1,*}, Yong Liu²

¹State Key Joint Laboratory of Environmental Simulation and Pollution Control,
College of Environmental Sciences and Engineering, Peking University, Beijing
100871, China

²Key Laboratory of Water and Sediment Sciences (Ministry of Education), College of
Environmental Sciences and Engineering, Peking University, Beijing 100871, China

* Corresponding author. Tel: 86-10-62751923. Email: xiesg@pku.edu.cn (S Xie)

22 **Abstract**

23 Lacustrine ecosystems are an important natural source of greenhouse gas methane.
24 Aerobic methanotrophs are regarded as a major regulator controlling methane
25 emission. Excess nutrient input can greatly influence carbon cycle in lacustrine
26 ecosystems. Ammonium is believed to be a major influential factor, due to its
27 competition with methane as the substrate for aerobic methanotrophs. To date, the
28 impact of ammonia on aerobic methanotrophs remains unclear. In the present study,
29 microcosms with freshwater lake sediment were constructed to investigate the
30 influence of ammonia concentration on aerobic methanotrophs. Ammonia influence
31 on the abundance of *pmoA* gene was only observed at a very high ammonia
32 concentration, while the number of *pmoA* transcripts was increased by the addition of
33 ammonium. *pmoA* gene and transcripts differed greatly in their abundance, diversity
34 and community compositions. *pmoA* transcripts were more sensitive to ammonium
35 amendment than *pmoA* gene. Methane oxidation potential and methanotrophic
36 community could be impacted by ammonium amendment. This work could add some
37 new sights towards the links between ammonia and methane oxidation in freshwater
38 sediment.

39

40 **Keywords:** Ammonium; Freshwater lake; Methane oxidation; Methanotroph; *pmoA*
41 gene; *pmoA* transcripts

42

43

44 **1. Introduction**

45 Methane is a major product of carbon metabolism in freshwater lakes, and also a
46 critical greenhouse gas in the atmosphere (Bastviken et al., 2004). Aerobic methane
47 oxidation performed by bacterial methanotrophs is a major pathway controlling
48 methane emission. Up to 30–99% of the total methane produced in anoxic sediment
49 can be oxidized by methanotrophs (Bastviken et al., 2008). **Therefore, aerobic**
50 **methane oxidation is an important biochemical process in freshwater lakes. And this**
51 **process** can be greatly influenced by the environmental changes (e.g. eutrophication)
52 induced by anthropogenic activities (Borrel et al., 2011).

53

54 The increasing input of nutrients into freshwater lakes has greatly raised the
55 availability of dissolved organic carbon (DOC), nitrogen and phosphorus, and also
56 exerted a considerable influence on aerobic methane oxidation (Liikanen and
57 Martikainen, 2003; Veraart et al., 2015). Among various types of nutrients,
58 ammonium, **an essential compound in nitrogen cycling**, has attracted great attention.
59 Ammonium and methane have similar chemical structure, and ammonium is known
60 to compete with methane for the binding site of methane monooxygenase, a key
61 enzyme in methane oxidation (Bédard and Knowles, 1989). On the other hand, a high
62 concentration of oxygen in lake water might also inhibit methane oxidation (Rudd and
63 Hamilton, 1975), and excess ammonium can lead to the competition between methane

64 oxidizers and ammonium oxidizers for oxygen. With high oxygen availability or low
65 in-situ nitrogen content, methane oxidation can also be stimulated by the addition of
66 ammonium (Rudd et al., 1976). Besides, ammonium might also induce differential
67 expression of pMMO encoding genes (Dam et al., 2014). Hence, the effect of
68 ammonium on methane oxidation in natural ecosystems is complex (Bodelier and
69 Laanbroek, 2004), and previous studies have documented contradictory results, such
70 as inhibition (Bosse et al., 1993; Murase and Sugimoto, 2005; Nold et al., 1999), no
71 effect (Liikanen and Martikainen, 2003), or stimulation (Bodelier et al., 2000; Rudd et
72 al., 1976). The effect of ammonium on methane oxidation might largely depend on
73 the characteristics of the studied ecosystem and in-situ environment (Bodelier and
74 Laanbroek, 2004; Borrel et al., 2011).

75
76 To date, previous studies about the ammonium effect on methane oxidation in
77 freshwater lakes mainly focused on either oxidation rate or net methane flux (Bosse et
78 al., 1993; Liikanen and Martikainen, 2003; Murase and Sugimoto, 2005). However,
79 methanotrophs play a fundamental role in regulating methane emission from
80 freshwater sediment (Bastviken et al., 2008). The abundance, transcription, and
81 community structure of aerobic methanotrophs may also be affected by the extra input
82 of ammonium (Shrestha et al., 2010). The difference in methanotrophic community
83 structure can further lead to various responses of methane oxidation to nitrogen
84 content (Jang et al., 2011; Mohanty et al., 2006; Nyerges and Stein, 2009).

85 Therefore, identification of the variation of methanotrophic community can be helpful
86 to understand how ammonium input influences methane oxidation process. The
87 community change of methanotrophs under ammonium stress has been observed in
88 various soils, such as agriculture soil (Seghers et al., 2003; Shrestha et al., 2010) and
89 landfill soil (Zhang et al., 2014). The results of these previous studies suggested that
90 the effect of ammonium on methanotroph community might be habitat-related. A
91 recent filed work suggested that in-situ ammonia concentration might be a key
92 regulating factor of methanotrophic community structure in freshwater lake sediment
93 (Yang et al., 2016). However, the direct evidence for the influence of ammonium (or
94 ammonia) on methanotroph community in freshwater lake sediment is still lacking.
95 Especially, many freshwater lakes in China have been suffering from eutrophication.
96 The methanotrophic communities in these ecosystems have been under high
97 ammonium pressure. The response pattern of methanotrophic community to
98 ammonium pressure in eutrophic lakes might be different from that in oligotrophic
99 lakes. Hence, in the present study, microcosms with eutrophic freshwater lake
100 sediment were constructed to investigate the ammonium influence on methane
101 oxidation potential and the abundance, transcription and community structure of
102 aerobic methanotrophs. The object of this current study was to demonstrate how
103 different concentrations of ammonium nitrogen impacted the structure and function of
104 aerobic methanotrophic communities in freshwater lakes with long-term
105 eutrophication.

106

107 **2. Materials and methods**

108 *2.1. Sediment characteristics*

109 Dianchi Lake is a large shallow lake (total surface area: 309 km²; average water
110 depth: 4.4 m) located in southeast China (Yang et al., 2016). This freshwater lake is
111 suffering from anthropogenically-accelerated eutrophication (Huang et al., 2017).

112 Surface sediment (0–5 cm) (24.9286N, 102.6582E) were collected using a core
113 sampler from the north part of Dianchi Lake in October, 2017. **The pH and water
114 dissolved oxygen (DO) were immediately measured with electrode sensors.**

115 **Ammonium nitrogen (NH₄⁺-N) was measured using Nessler's reagent
116 spectrophotometric method. Physicochemical properties of sediment were determined
117 according to the literature (Wang, 2012).** In-situ dissolved oxygen (DO) and

118 ammonium nitrogen (NH₄⁺-N) in overlying water were 8.37 mg/L and 344 μM,
119 respectively. Sediment total organic carbon (TOC), total nitrogen (TN), the ratio of
120 TOC to TN (C/N), nitrate nitrogen (NO₃⁻-N), ammonium nitrogen (NH₄⁺-N), total
121 phosphorus (TP), and pH were 41.3 g/kg, 3.95 g/kg, 10.5, 12.3 mg/kg, 364 mg/kg,
122 0.60 g/kg, and 7.2, respectively. Sediment (2 L) was transported to laboratory at 4°C
123 for incubation experiment.

124

125 *2.2. Experimental setup*

126 Sediments were placed at room temperature for 24 h and then homogenized. The
127 homogenized sediments were centrifuged at 5000 rpm for 10 min to determine the
128 initial ammonia concentration of pore water. A series of 50-mL serum bottles (as
129 microcosms) were added with 10 mL of sediment aliquot (containing about 0.1 g dry
130 sediment). A total of 111 microcosms were constructed, including three autoclaved
131 ones used as the control for the measurement of methane oxidation potential. Six
132 treatments (A–F) were set up. The microcosms with treatments B–F were added with
133 1 mL of NH₄Cl at the levels of 5, 20, 50, 100, and 200 mM, respectively, while the
134 microcosm with treatment A was amended with 1 mL diluted water as the blank
135 control. For each treatment, 18 microcosms were constructed, including half used for
136 molecular analyses and another half for methanotrophic potential measurement. These
137 microcosms were closed with butyl rubber stoppers and incubated for 14 days at 25°C
138 at 100 rpm in dark.

139

140 At each sampling time point (day 1 (12 h after incubation), day 7 or day 14), triplicate
141 sediment samples of each treatment were transferred into Falcon tubes, and then
142 centrifuged at 5000 rpm for 10 min. The supernatant was filtered with a 0.2- μ m
143 syringe filter, and its ammonia level was measured using Nessler reagent-colorimetry.
144 The sediment was mixed up and immediately used for nucleic acid extraction. In
145 addition, at each sampling time, for methanotrophic potential measurement, another
146 three bottles of each treatment were opened and shaken to provide ambient air, then

147 closed again with butyl rubber stoppers. Headspace air (1 mL) was replaced by CH₄
148 (99.99%) with an air-tight syringe. Samples were shaken vigorously to mix. After
149 incubation at 25°C, 100 rpm for 24 h, 0.1 mL of headspace gas was taken and
150 measured using a GC126 gas chromatograph equipped with a flame ionization
151 detector. Autoclaved control was also processed to exclude methane loss due to
152 dissolution or airtightness.

153

154 *2.3. Nucleic acid extraction, reverse transcription and quantification*

155 Sediment DNA and RNA were extracted with PowerSoil DNA Isolation Kit (MoBio)
156 and PowerSoil Total RNA Isolation Kit (MoBio, USA), respectively. The quality and
157 concentration of extracted nucleic acids were examined with Nanodrop 2000 (Thermo
158 Fisher Scientific, USA). RNA was diluted to a similar concentration before further
159 analysis. Real-time PCR of *pmoA* gene was performed on a CFX Connect cycler
160 (Bio-Rad, USA), using the primer set A189f/mb661r following the conditions
161 reported in our previous study (Liu et al., 2015). Reactions were carried out using a
162 TransStart Top Green qPCR Kit (Transgen, China) following the manufacturer's
163 instructions. Gene transcripts were quantified in a one-step RT-qPCR using a
164 TransScript Green One-step qRT-PCR Kit. Melting curve analyses were carried out at
165 the end of PCR run to check the amplification specificity. Each measurement was
166 carried out with three technical replicates. Standard curve was constructed with *pmoA*
167 gene clones, and the efficiency and r-square were 91.5% and 0.998, respectively.

168

169 *2.4. Terminal restriction fragment length polymorphism (T-RFLP) fingerprinting*

170 DNA *pmoA* gene fragment was amplified with primer sets A189f/mb661r, with the
171 forward primer A189f modified with FAM at 5'-end. PCR reactions were performed
172 as previously described (Liu et al., 2015). Two-step RT-PCR was carried out on
173 RNA. In the first step, RNA was reversely transcribed into cDNA with *pmoA* gene
174 specific primer using One-step gDNA removal and cDNA synthesis kit (Transgen
175 Biotech Co., LTD, China). The 20- μ L reaction solution contained 1 μ L EasyScript
176 RT/RI Enzyme Mix, 1 μ L gDNA remover, 10 μ L 2 \times ES Reaction Mix, 2 pmol of gene
177 specific primers and 1 μ L RNA template. The reaction mixture was incubated at 42°C
178 for 30 min, and the enzymes were deactivated at 85°C for 5 s. In the second step, 1 μ L
179 cDNA was used as template in *pmoA* gene PCR amplification, proceeded following
180 the same protocol with DNA.

181

182 The fluorescently labeled PCR products were purified using a TIANquick Mini
183 Purification Kit (TIANGEN Bitotech Co., Ltd, China). Approximately 20 ng of
184 purified PCR products were digested with restriction endonuclease *Bci*T130 I (Takara
185 Bio Inc., Japan) following the conditions recommended by the manufacturer's
186 instruction. Electrophoresis of digested amplicons was carried out by Sangon Biotech
187 (China) using an ABI 3730 DNA analyzer (Thermo Fisher Scientific, USA). The
188 length of T-RFs was determined by comparing with internal standard using the

189 GeneScan software. Terminal restriction fragments (T-RFs) with similar length (less
190 than 2 bp difference) were merged, and T-RFs shorter than 50 base pairs (bp) or
191 longer than 508 bp were removed from the dataset. Relative abundance of each
192 fragment equaled to the ratio of its peak area to the total area. Minor T-RFs with
193 relative abundance less than 0.5 % were excluded for further analysis. The Shannon
194 diversity indices of *pmoA* gene and transcripts were calculated based on DNA and
195 RNA T-RFs, respectively.

196

197 *2.5. Cloning, sequencing and phylogenetic analysis*

198 *pmoA* gene clone library was generated with mixed DNA PCR products using a TA
199 cloning kit (TransGen Biotech Co., LTD, China). Randomly picked clones were
200 subjected to sequencing. **A total of 93 *pmoA* sequences were retrieved and** in silico
201 cut sites of these *pmoA* sequences were predicted using the online software
202 Restriction Mapper (<http://www.restrictionmapper.org>). **Several** sequences of each T-
203 RF, together with their reference sequences from the GenBank database, were used
204 for phylogenetic analysis. A neighbor-joining tree was conducted with MEGA 7
205 (Kumar et al., 2016), and bootstrap with 1000 replicates was carried out to check the
206 consistency. The phylogenetic tree was visualized using iTOL v4.2 (Letunic and
207 Bork, 2016). The sequences used in phylogenetic analysis were deposited in GenBank
208 database, and the accessions were shown in Fig. 3.

209

210 2.6. Statistical analysis

211 Two-way ANOVA (analysis of variance) was carried out to determine the effect of
212 ammonia concentration and incubation time on CH₄ oxidation potential, gene
213 abundance and transcription. One-way ANOVA followed by Student-Newman-Keuls
214 test was adopted to detect the difference among treatments. The analysis was carried
215 out in *R*, using *R* packages stats (version 3.4.4) and agricolae (version 1.2-8).
216 Moreover, the comparison of methanotrophic communities in different microcosms,
217 using Redundancy Analysis (RDA) and clustering analysis, was carried out with *R*
218 package Vegan (version 2.4-6) (Oksanen et al., 2018). Permutation test was carried
219 out to detect the margin effect of variables (treatment and time). Clustering analysis
220 was carried out based on Bray-Curtis dissimilarity, to demonstrate the variation of
221 microbial community structure during incubation.

222

223 3. Results

224 3.1. Methane oxidation potential

225 Ammonium was found to quickly deplete in each ammonium added microcosm (Fig.
226 S1). Methane oxidation potential (MOP) varied from 0.77 (in the microcosm F with
227 200 mM ammonium on day 1) to 1.94 (in the microcosm F with 200 mM ammonium
228 on day 14) mmol/g dry sediment day (Fig. 1), while autoclaved control did not show
229 notable methane oxidation (data not shown). Based on two-way ANOVA, both
230 ammonium concentration (treatment) and incubation time had significant effects on

231 MOP ($P < 0.01$), and their interaction was also significant ($P < 0.05$). The MOP in the
232 microcosm with treatment A (with no external ammonium addition) did not show a
233 significant difference among incubation times ($P > 0.05$). Based on post-hoc test (Fig.
234 1, Table S1), at each time, the microcosm with **treatment B (5 mM ammonium)** had
235 slightly higher MOP than the microcosm with control group (A). At days 1 and 7, the
236 microcosms with **20-100 mM ammonium addition** had slightly lower MOP than the
237 un-amended microcosm. However, at each time, no statistical difference in MOP was
238 observed among the microcosms with **treatment A-E (0-100 mM ammonium**
239 **addition)**. Moreover, the microcosm with treatment F (**200 mM ammonium**) tended to
240 have significantly lower MOP than other microcosms on day 1 ($P < 0.05$), but
241 significantly higher MOP on day 14 ($P < 0.05$). On day 7, no statistical difference in
242 MOP was found between the microcosm with treatment F and any other microcosms.

243

244 3.2. *pmoA* gene and transcript abundance

245 Two-way ANOVA indicated that the number of both *pmoA* gene and transcripts was
246 significantly influenced by ammonium concentration and incubation time ($P < 0.01$)
247 (Fig. 2a and 2b). The abundance of *pmoA* gene in the **control group (A)** showed no
248 significant difference among times ($0.05 < P < 0.1$). On day 1, the microcosms with
249 treatment C and D (**20-100 mM ammonium**) had higher (but not significantly) *pmoA*
250 gene abundance than other microcosms. However, at days 7 and 14, the microcosm

251 with treatment F (with the highest ammonium addition of 200 mM) had the highest
252 *pmoA* gene abundance.

253

254 At each time, *pmoA* transcripts in the un-amended microcosm was less abundant than
255 those in amended microcosms. On day 1, the highest number of transcripts was
256 observed in the microcosm with treatment C (20 mM), followed by the microcosms
257 with treatments D, E and F (50-200 mM). The microcosm with treatment B (5 mM)
258 had much lower *pmoA* transcript abundance than other ammonium added microcosms
259 ($P < 0.05$) (Table S1). On day 7, *pmoA* transcript abundance tended to increase with
260 the level of added ammonium, although statistical difference in *pmoA* transcript
261 abundance was only observed between treatment F and other treatments. On day 14,
262 no significant difference in *pmoA* transcript abundance was detected among
263 treatments ($P > 0.05$).

264

265 The ratio of transcripts to *pmoA* gene varied with ammonium concentration and
266 incubation time (Fig. S2). The ratio tended to decrease with time in ammonium
267 amended microcosms. Moreover, at days 1 and 7, the ratio tended to increase with the
268 increasing ammonium concentration.

269

270 3.3. *T-RFLP* fingerprinting

271 In silico analysis of the cloned *pmoA* sequences showed that restriction enzyme
272 *BciTI30* I could well capture *pmoA* gene diversity and present a good resolution
273 among different subgroups of aerobic methanotrophs. Most of the T-RFs retrieved in
274 the current study could be assigned to certain methanotrophic groups, while some of
275 the T-RFs from *pmoA* transcripts could not match the cut site predicted from the
276 sequences in clone library. The obtained *pmoA* sequences could be grouped into four
277 clusters (Fig. 3), which could be convincingly affiliated with known methanotrophic
278 organisms. Three clusters were affiliated with Type I methanotrophs
279 (*Gammaproteobacteria*), which could be further divided into several subgroups.
280 Cluster 1 contained 157 bp, 242 bp and 338 bp T-RFs that could be related to Type Ia
281 methanotrophs, the most frequently detected methanotrophs in freshwater lakes
282 (Borrel et al., 2011). The 157 bp and 338 bp T-RFs might be affiliated with
283 *Methylobacter* and *Methylomicrobium*, respectively. However, the 242 bp T-RF could
284 not be convincingly assigned to a certain genus because of the highly similar *pmoA*
285 sequences of Type Ia organisms. Cluster 2 was composed of three different T-RFs,
286 and could be affiliated with *Methylococcus* and *Methyloparacoccus*. Cluster 3
287 included the T-RFs of 91 bp and 508 bp, which might be closely related to
288 *Candidatus Methylospira*. Both cluster 2 and cluster 3 could be affiliated with Type
289 Ib methanotrophs, but they distinctly differed in phylogeny and morphology
290 (Danilova et al., 2016). Cluster 4 comprised of the T-RFs of 217 bp, 370 bp and 403
291 bp, and it was phylogenetically related to Type IIa methanotrophs (*Methylocystaceae*

292 in *Alphaproteobacteria*). The 403 bp T-RF was likely affiliated with *Methylosinus*,
293 while 217 bp and 370 bp T-RFs could not be convincingly assigned to a single genus.

294

295 The 508 bp fragment could be affiliated with either *Methylospira* or unknown Type Ia
296 methanotroph. Considering the low abundance of 508 bp T-RF (<0.5% in DNA
297 TRFLP profile and approximately 2% in RNA TRFLP profile), and in order to avoid
298 incorrect annotation, this T-RF was excluded from further analysis.

299

300 3.4. T-RFLP diversity and profiles of *pmoA* gene and transcripts

301 Diversity of each community was calculated based on T-RFLP results. In the current
302 study, the T-RFs with relative abundance more than 5% in at least one sample or with
303 average relative abundance more than 2% in all samples were defined as major T-
304 RFs. For a given sample, the total number of T-RFs and the number of major T-RFs
305 were greater in RNA T-RFLP profile than in DNA T-RFLP profile. On day 1,
306 ammonium amended microcosms tended to have lower *pmoA* gene diversity than un-
307 amended microcosm, while an opposite trend was found at days 7 and 14 (Table 1).
308 For a given sample, *pmoA* transcript showed higher Shannon diversity than *pmoA*
309 gene. Ammonium amended microcosms tended to have lower *pmoA* transcript
310 diversity than un-amended microcosm. In the microcosms with treatments A–D (0-50
311 mM ammonium), *pmoA* transcript diversity tended to increase with time. However,

312 the Shannon diversity of transcriptional T-RFs experienced an increase followed by a
313 decrease in the microcosms with treatments E and F (100-200 mM ammonium).

314

315 A total of 11–14 T-RFs were retrieved from T-RFLP analysis of DNA samples. Most
316 of them (including all major T-RFs) could be well assigned to certain methanotrophic
317 groups (Figs. 3 and 4a). In all DNA samples, Type Ia and Type IIa methanotrophs
318 dominated methanotrophic communities. On day 1, the 242 bp T-RF (*Methylobacter*-
319 related Type Ia methanotrophs) comprised about 50% of methanotrophic
320 communities. The 370 bp T-RF (Type IIa methanotrophs) also showed a considerable
321 proportion (20–25%). The addition of ammonium tended to induce no considerable
322 change of methanotrophic community structure after 12-hour incubation. After 7 and
323 14 days of incubation, the proportions of major T-RFs illustrated an evident variation.
324 The proportion of Type Ia methanotrophs (157 bp, 242 bp and 338 bp; marked in
325 green) decreased with time, while Type IIa methanotrophs (217 bp and 370 bp,
326 marked in pink) increased. The proportion of *Methylococcus*-related Type Ib
327 methanotrophs (marked in blue) also increased, especially the 145 bp T-RF, whereas
328 the proportion of *Methylospira*-related Type Ib methanotrophs (91 bp, marked in
329 yellow) did not show a notable variation.

330

331 A total of 14–38 T-RFs were retrieved from T-RFLP analysis of RNA samples, but
332 most of them were only detected in a few samples with low relative abundance (Fig.

333 4b). Among the major transcript T-RFs, only 4 transcript T-RFs could be assigned to
334 a known methanotrophic group, and on day 1 they comprised of a considerable part of
335 methanotrophic community in un-amended microcosm (43–72%) and of in amended
336 microcosms (22–72%), while the other 7 T-RFs were not found in *pmoA* gene library
337 as well as DNA T-RFLP profiles. Compared with *pmoA* gene, the community
338 structure of *pmoA* transcripts was more sensitive to external ammonium addition. The
339 addition of ammonium induced a marked shift in *pmoA* transcriptional community
340 structure after 12-h incubation. The proportion of 242 bp increased, but the proportion
341 of 91 bp decreased. After 1 or 2 weeks' incubation, the microcosms with treatments
342 B, C, D and E (5-100 mM ammonium) had similar transcriptional community
343 structure as the un-amended microcosm. However, the microcosm with treatment F
344 (with the highest ammonium addition) encountered a remarkable increase in 91 bp
345 (Ca. *Methylospira*-related Type Ib methanotrophs). Moreover, the 370 bp T-RF,
346 accounting for up to one fourth (average) of DNA T-RFs, was only detected on day
347 14, with relative abundance of 0.8–2.9%.

348

349 3.5. Clustering and statistical analysis of TRFLP profiles

350 DNA- and RNA-based methanotrophic community structures were characterized with
351 hierarchal clustering based on Bray-Curtis dissimilarity (Fig. 5). *pmoA* community
352 structure was quite stable during the whole incubation period. Most of the samples on

353 day 1 were grouped together. Samples B7, D7, E7, B14, C14, D14, E14 and F14 were
354 clustered into another group. Sample D1 was distantly separated from other samples,
355
356 Higher dissimilarity of transcriptional community structures could be observed among
357 samples. The samples on day 1 were still close to each other, and they were clearly
358 separated from the samples at day 7 and 14. Samples A7, A14, B7, B14, D7, E7 and
359 F7 could form a clade, while samples C7, D14 and E14 formed another clade.
360 Moreover, sample F14 was distantly separated from other samples.

361

362 RDA with permutation test was carried out to test the potential relationship between
363 each major T-RF and factors (treatment and incubation time). The result indicated that
364 incubation time had a significant impact on DNA-based methantrophic community
365 composition ($P < 0.01$), while ammonium concentration did not exert a significant
366 influence ($P > 0.05$). The constrained variables could explain up to 74.4 % of total
367 variance. However, most of the explained variance (73.7% out of 74.4%) was related
368 to constrained axis 1, and only the first axis was significant ($P = 0.029$). In addition,
369 for RNA-based methantrophic community, treatment and time were able to explain
370 76.0% of total variance. Only incubation time had a significant effect on RNA-based
371 methantrophic community composition ($P < 0.01$), and only the first constrained axis
372 was significant ($P < 0.01$). These results indicated that after the addition and with the

373 depletion of ammonium, the community compositions of both *pmoA* gene and
374 transcripts could undergo a considerable shift.

375

376 **4. Discussion**

377 *4.1. Effect of ammonium on MOP*

378 The current study showed that a high dosage of ammonium could present a temporary
379 inhibition effect on methane oxidation. The result was consistent with several
380 previous studies (Bosse et al., 1993; Murase and Sugimoto, 2005; Nold et al., 1999).

381 These studies indicated that the addition of ammonium might inhibit methane
382 oxidation in water and sediment of freshwater lake. However, to date, the minimal
383 inhibit concentration for methane oxidation in lake sediment is still unclear. Bosse et
384 al. (1993) pointed out that methane oxidation in littoral sediment of Lake Constance
385 could be partially inhibited when ammonium concentration in pore water was higher
386 than 4 mM. In contrast, methane oxidation in sediment of hyper-eutrophic Lake
387 Kevätön was not obviously affected by a continuous water flow containing up to 15
388 mM of ammonium (Liikanen and Martikainen, 2003). Lake Kevätön and Dianchi
389 Lake had similar average water depth, and the overlying water of sediment in both
390 lakes had very high levels of ammonium (Liikanen and Martikainen, 2003). In the
391 present study, inhibition was only observed in the microcosm with a very high
392 ammonium dosage (with 17.3 mM ammonium in overlying water on day 1), while no
393 evident inhibition was found in the other ammonium amended microcosms, even at

394 high dosages. This suggested that methane oxidation might depend on ammonium
395 dosage, which was sustained by the result of two-way ANOVA. The minimal inhibit
396 concentration for methane oxidation in Dianchi Lake was much higher than that in
397 Lake Constance (Bosse et al. 1993). Hence, the minimal inhibition concentration for
398 methane oxidation could be lake-specific.

399

400 Despite of a very high dosage of ammonium, sediment MOP was only partially
401 inhibited. This might be explained by two facts. The studied sediment sample
402 originated from a eutrophic lake, which suffered from high ammonium input.
403 Methanotrophs in this kind of ecosystem could effectively oxidize methane under the
404 condition of high ammonia concentration (Liikanen and Martikainen, 2003). This was
405 consistent with the above-mentioned lake-related minimal inhibition concentration for
406 methane oxidation. On the other hand, the affinity of pMMO (*pmoA* encoding
407 protein) to methane is much higher than that to ammonium (Bédard and Knowles,
408 1989). As a result, when the methane concentration is high enough, as a common case
409 for the measurement of MOP, methanotrophs should be able to consume a
410 considerable amount of methane.

411

412 A recovery of MOP after a single-shot fertilization has been reported in forest soil
413 (Borjesson and Nohrstedt, 2000). In this study, it was noted that after the depletion of
414 ammonium, sediment MOP could also get a quick recovery. The highest ammonium

415 dosage eventually stimulated sediment MOP in the long run (about two weeks).
416 Considering the increase of *pmoA* gene abundance and the change of RNA-based
417 methanotrophic community structure, this might be attributed to an adaption to the
418 environment. The initial decrease of MOP could be explained by the competition
419 between methane and ammonium for pMMO (Bédard and Knowles, 1989), while the
420 subsequent increase of MOP might be the consequence of the shift in methanotrophic
421 community structure (Seghers et al., 2003; Shrestha et al., 2010) and the increase of
422 *pmoA* gene abundance and transcription.

423

424 4.2. *Effect of ammonium on pmoA gene and transcript abundance*

425 So far, little is known about the changes of methanotrophic abundance and transcripts
426 induced by external ammonium amendment. Alam and Jia (2012) reported that the
427 addition of 200 µg of nitrogen/g dry weight soil (in ammonium sulfate) showed no
428 significant influence on *pmoA* gene abundance in paddy soil. However, in
429 ammonium-amended rhizospheric soil microcosms, *pmoA* gene abundance slightly
430 increased after 29 days' incubation (Shrestha et al., 2010). In this study, after 7 days'
431 incubation, the sediment microcosm with the highest ammonium dosage had much
432 higher *pmoA* gene abundance than un-amended microcosm and other amended
433 microcosms with lower dosage, whereas no significant difference of *pmoA* gene
434 abundance was detected between un-amended microcosm and amended microcosms
435 (except for the treatment with the highest ammonium dosage). After 14 days'

436 incubation, the microcosm with the highest ammonium dosage also had much higher
437 DNA-based methanotrophic abundance than other amended microcosms. Hence, the
438 present study further provided the evidence that the addition of ammonium,
439 depending on dosage, could influence freshwater sediment DNA-based
440 methanotrophic abundance, which was in agreement with the result of two-way
441 ANOVA. Dianchi Lake had been suffering from eutrophication for over 30 years
442 (Huang et al., 2017). It could be assumed that methanotroph community in this lake
443 had been adapted to high in-situ ammonia concentration. As a result, only extremely
444 high dosage of ammonium could pose a significant impact on DNA-based
445 methanotrophic abundance.

446

447 At each time, the microcosm with no external ammonium addition had lower
448 abundance of *pmoA* transcripts than each amended microcosm. This suggested the
449 addition of ammonium could influence the transcription of *pmoA* gene. The
450 stimulation of *pmoA* transcription by the addition of ammonium could be attributed to
451 the competition between methane and ammonium for the binding site of pMMO
452 (Bédard and Knowles, 1989). This was also verified by the similar number of
453 transcripts in these amended microcosms after the considerable reduction of
454 ammonium. At days 1 and 14, the abundance of *pmoA* transcripts differed greatly in
455 different amended microcosms. This suggested that ammonium dosage could

456 influence the number of *pmoA* transcripts, which was consistent with the result of
457 two-way ANOVA.

458

459 *4.3. Effect of ammonium on DNA- and RNA-based methanotrophic community*
460 *compositions*

461 Several previous studies have investigated the influence of ammonium amendment on
462 soil methanotrophic community structure (Alam and Jia, 2012; Mohanty et al., 2006;
463 Shrestha et al., 2010), yet information about the influence of ammonium amendment
464 on freshwater methanotrophic community structure is still lacking. In this study,
465 immediately after ammonium addition (after 12-h incubation), the relative abundance
466 of Type I (especially Type Ia) methanotrophs transcripts increased, instead of Type II.
467 This coincided with the result reported in rice and forest soils (Mohanty et al., 2006).
468 This also suggested that a high level of ammonia favored the growth of Type I
469 methanotrophs and they might play an important role in methane oxidation in
470 ammonia-rich lake. However, both DNA- and RNA-based T-RFLP profiles indicated
471 that the addition of ammonium lead to an increase in the ratio of Type II to Type I
472 methanotrophs in two weeks, which was contrary to the results observed in some
473 previous studies in soil ecosystems (Alam and Jia, 2012; Bodelier et al., 2000;
474 Mohanty et al., 2006). These previous studies found that Type I methanotrophs had a
475 numerical advantage over Type II at a high ammonia concentration. Our recent field
476 study suggested that that the abundance of Type II methanotrophs in sediment of

477 Dianchi Lake was closely correlated to the concentration of ammonia (Yang et al.,
478 2016). Therefore, the response of methanotrophs to ammonia might depend on the
479 type of ecosystem. In addition, the community compositions of *pmoA* genes and
480 transcripts could be divergent, and DNA-based and RNA-based methanotrophs could
481 show different responses to ammonium addition (Shrestha et al. 2010). In this study,
482 compared with *pmoA* gene, the community structure of *pmoA* transcripts was more
483 sensitive to external ammonium addition. This was in a consensus with the result of a
484 previous study on the effect of ammonium addition on methanotrophs in root and
485 rhizospheric soils (Shrestha et al. 2010).

486

487 *4.4 TRFLP fingerprinting*

488 T-RFLP has been a popular approach to capture microbial community diversity. It has
489 been also widely used in community studies of methylotrophs (Mohanty et al., 2006;
490 Pester et al., 2004; Shrestha et al., 2010). However, the most widely used digestive
491 enzyme, *MspI*, may not be suitable for all kinds of samples. For example, samples
492 from littoral Lake Constance only resulted in a few T-RFs. And most of the clones
493 from Type I were at the same T-RF length of 248 bp (Pester et al., 2004). *MspI*
494 enzyme also generated only very few T-RFs for the sediment samples from Dianchi
495 Lake. The number of T-RFs based on a certain digestive enzyme might partly depend
496 on the in-situ microbial community features. Since T-RF was only related to the first
497 cleavage site, if a specific point mutation got widespread (especially when the

498 population was limited), it might notably impact the T-RF pattern. Efforts were made
499 to avoid some of the weakness of T-RFLP and improve the taxonomic resolution,
500 including the application of multiplex T-RFLP (Elliott et al., 2012) and the usage of
501 primers labelled with different fluorochromes (Deutzmann et al., 2011). Here, we
502 tried to choose a suitable enzyme based on in-silico analysis. A previous NGS result
503 of methylotrophic community in the same region (under accession number
504 SRP131884) was used as a reference. The *pmoA* sequences were grouped into OTUs
505 at 0.03 cutoff, and the representative sequences of each OTU were used in mapping.
506 We tested all the enzymes listed in <http://www.restrictionmapper.org>, and calculated
507 the proportion of each T-RF. A simplified T-RF map (including the enzymes which
508 could cut over 80% of total sequences) was shown in Fig S3. We expected that a good
509 digestive enzyme should: (1) generate no or few T-RFs smaller than 50 bp or larger
510 than 500 bp; (2) generate T-RFs having at least 2 bp differences among each other; (3)
511 generate more T-RFs to retrieve the diversity; (4) be consistent with taxon and
512 phylogenetic tree (i.e., the same T-RF should not be affiliated to very distantly related
513 taxa). Based on these rules, most of the enzymes were easy to exclude. *MspI* and
514 *BciT130I*, the same as *HpaII* and *EcoRII*, respectively, were further tested using a
515 neighbor-joining tree. *BciT130I* was able to generate more different T-RFs, and thus
516 could more ideally reflect methylotrophic diversity. It also had a better taxonomic
517 resolution than *MspI*.

518

519

520 **5. Conclusions**

521 This was the first microcosm study on the influence of ammonium on freshwater lake
522 sediment methanotroph community. In freshwater lake sediment microcosm, methane
523 oxidation potential and methanotrophic community could be influenced by
524 ammonium amendment. Ammonia concentration had a significant impact on
525 methanotrophic abundance and diversity, but exerted no evident influence on
526 community structure. Compared with *pmoA* gene, transcripts were more sensitive to
527 external ammonium addition. Further works are necessary in order to elucidate the
528 influence of ammonium on methane oxidation in freshwater sediment.

529

530 **Conflict of interest**

531 The authors declare that they have no competing interests.

532

533 **Acknowledgments**

534 This work was financially supported by National Natural Science Foundation of
535 China (No. 41571444), and National Basic Research Program of China (No.
536 2015CB458900).

537

538 **References**

539 Alam, M., Jia, Z., 2012. Inhibition of methane oxidation by nitrogenous fertilizers in a

540 paddy soil. *Front. Microbiol.* 3, 246.

541 Bastviken, D., Cole, J., Pace, M., Tranvik, L., 2004. Methane emissions from lakes:
542 Dependence of lake characteristics, two regional assessments, and a global
543 estimate. *Glob. Biogeochem. Cycle* 18, GB4009.

544 Bastviken, D., Cole, J., Pace, M., de Bogert, M., 2008. Fates of methane from
545 different lake habitats: Connecting whole-lake budgets and CH₄ emissions. *J.*
546 *Geophys. Res.-Biogeosci.* 113, G02024.

547 Bédard, C., Knowles, R., 1989. Physiology, biochemistry, and specific inhibitors of
548 CH₄, NH₄⁺, and CO oxidation by methanotrophs and nitrifiers. *Microbiol. Rev.* 53,
549 68–84.

550 Bodelier, P.L.E., Roslev, P., Henckel, T., Frenzel, P., 2000. Stimulation by ammonium-
551 based fertilizers of methane oxidation in soil around rice roots. *Nature* 403, 421–
552 424.

553 Bodelier, P.L.E., Laanbroek, H.J., 2004. Nitrogen as a regulatory factor of methane
554 oxidation in soils and sediments. *FEMS Microbiol. Ecol.* 47, 265–277

555 Borjesson, G., Nohrstedt, H.O., 2000. Fast recovery of atmospheric methane
556 consumption in a Swedish forest soil after single-shot N-fertilization. *For. Ecol.*
557 *Manage.* 134, 83–88.

558 Borrel, G., Jezequel, D., Biderre-Petit, C., Morel-Desrosiers, N., Morel, J.P., Peyret,
559 P., Fonty, G., Lehours, A.C., 2011. Production and consumption of methane in
560 freshwater lake ecosystems. *Res. Microbiol.* 162, 832–847.

561 Bosse, U., Frenzel, P., Conrad, R., 1993. Inhibition of methane oxidation by
562 ammonium in the surface layer of a littoral sediment. FEMS Microbiol. Ecol. 13,
563 123–134.

564 Dam, B., Dam, S., Kim, Y., Liesack, W., 2014. Ammonium induces differential
565 expression of methane and nitrogen metabolism-related genes in *Methylocystis* sp.
566 strain SC2, Environ. Microbiol. 16, 3115–3127.

567 Danilova, O.V., Suzina, N.E., Van De Kamp, J., Svenning, M.M., Bodrossy, L.,
568 Dedysh, S.N., 2016. A new cell morphotype among methane oxidizers, a spiral-
569 shaped obligately microaerophilic methanotroph from northern low-oxygen
570 environments. ISME J. 10, 2734–2743.

571 Deutzmann, J. S. S., Wörner, S. and Schink, B., 2011. Activity and diversity of
572 methanotrophic bacteria at methane seeps in eastern Lake Constance sediments,
573 Appl. Environ. Microbiol. 77, 2573-2581.

574 Elliott, G., Thomas, N., MacRae, M., Campbell, C., Ogden, I., Singh, B., 2012.
575 Multiplex T-RFLP Allows for increased target number and specificity: Detection of
576 *Salmonella enterica* and six species of *Listeria* in a single test. Plos One, 7, e43672.

577 Jang, I., Lee, S., Zoh, K.D., Kang, H., 2011. Methane concentrations and
578 methanotrophic community structure influence the response of soil methane
579 oxidation to nitrogen content in a temperate forest. Soil Biol. Biochem. 43, 620–
580 627.

581 Huang, C.C., Yao, L., Zhang, Y.L., Huang, T., Zhang, M.L., Zhu, A.X., Yang, H.,

582 2017. Spatial and temporal variation in autochthonous and allochthonous
583 contributors to increased organic carbon and nitrogen burial in a plateau lake. *Sci.*
584 *Total Environ.* 603, 390–400.

585 Kumar, S., Stecher, G., Tamura, K., 2016. MEGA7: Molecular evolutionary genetics
586 analysis version 7.0 for bigger datasets. *Mol. Biol. Evol.* 33, 1870–1874.

587 Letunic, I., Bork, P., 2016. Interactive tree of life (iTOL) v3, an online tool for the
588 display and annotation of phylogenetic and other trees. *Nucleic Acids Res.* 44,
589 W242–W245.

590 Liikanen, A., Martikainen, P.J., 2003. Effect of ammonium and oxygen on methane
591 and nitrous oxide fluxes across sediment–water interface in a eutrophic lake.
592 *Chemosphere* 52, 1287–1293.

593 Liu, Y., Zhang, J.X., Zhao, L., Li, Y.Z., Yang, Y.Y., Xie, S.G., 2015. Aerobic and
594 nitrite-dependent methane-oxidizing microorganisms in sediments of freshwater
595 lakes on the Yunnan Plateau. *Appl. Microbiol. Biotechnol.* 99, 2371–2381.

596 Mohanty, S.R., Bodelier, P.L., Floris, V., Conrad, R., 2006. Differential effects of
597 nitrogenous fertilizers on methane-consuming microbes in rice field and forest
598 soils. *Appl. Environ. Microbiol.* 72, 1346–1354.

599 Murase, J., Sugimoto, A., 2005. Inhibitory effect of light on methane oxidation in the
600 pelagic water column of a mesotrophic lake (Lake Biwa, Japan). *Limnol.*
601 *Oceanogr.* 50, 1339–1343.

602 Nold, S.C., Boschker, H.T.S., Pel, R., Laanbroek, H.J., 1999. Ammonium addition
603 inhibits ¹³C-methane incorporation into methanotroph membrane lipids in a
604 freshwater sediment. *FEMS Microbiol. Ecol.* 29, 81–89.

605 Nyerges, G., Stein, L.Y., 2009. Ammonia cometabolism and product inhibition vary
606 considerably among species of methanotrophic bacteria. *FEMS Microbiol. Lett.*
607 297, 131–136.

608 Oksanen, J., Blanchet, F.G., Friendly, M., Kindt, R., Legendre P., McGlenn, D.,
609 Minchin, P.R., O'Hara, R. B., Simpson G.L, Solymos, P., Stevens M.H.H.,
610 Szoecs, E., Wagner, H., 2018. Vegan, Community ecology package, version 2.4-
611 6, Available at, <https://CRAN.R-project.org/package=vegan>.

612 Pester, M., Friedrich, M., Schink, B., Brune, A., 2004. *pmoA*-based analysis of
613 methanotrophs in a littoral lake sediment reveals a diverse and stable community
614 in a dynamic environment, *Appl. Environ. Microbiol.* 70, 3138-3142.

615 Rudd, J.W.M., Hamilton, R.D., 1975. Factors controlling rates of methane oxidation
616 and the distribution of the methane oxidizers in a small stratified lake. *Arch.*
617 *Hydrobiol.* 75, 522–538.

618 Rudd, J.W.M., Furutani, A., Flett, R.J., Hamilton, R.D., 1976. Factors controlling
619 methane oxidation in Shield Lakes: The role of nitrogen fixation and oxygen
620 concentration. *Limnol Oceanogr*, 21, 357–364.

621 Seghers, D., Top, E.M., Reheul, D., Bulcke, R., Boeckx, P., Verstraete, W., Siciliano,
622 S.D., 2003. Long-term effects of mineral versus organic fertilizers on activity

623 and structure of the methanotrophic community in agricultural soils. *Environ.*
624 *Microbiol.* 5, 867–877.

625 Shrestha, M., Shrestha, P.M., Frenzel, P., Conrad, R., 2010. Effect of nitrogen
626 fertilization on methane oxidation, abundance, community structure, and gene
627 expression of methanotrophs in the rice rhizosphere. *ISME J* 4, 1545–1556.

628 Veraart, A.J., Steenbergh, A.K., Ho, A., Kim, S.Y., Bodelier, P.L.E., 2015. Beyond
629 nitrogen: The importance of phosphorus for CH₄ oxidation in soils and
630 sediments. *Geoderma* 259, 337–346.

631 Wang, S. H., 2012. *Manual for sediment mass investigation and assessment.* Science
632 Press, Beijing.

633 Yang, Y.Y., Zhao, Q., Cui, Y.H., Wang, Y.L., Xie, S.G., Liu, Y., 2016. Spatio-
634 temporal variation of sediment methanotrophic microorganisms in a large
635 eutrophic lake. *Microb. Ecol.* 71, 9–17.

636 Zhang, X., Kong, J.Y., Xia, F.F., Su, Y., He, R., 2014. Effects of ammonium on the
637 activity and community of methanotrophs in landfill biocover soils. *Syst. Appl.*
638 *Microbiol.* 37, 296–304.

639

640

641

642

643

644

645

646

647 **Table 1** Numbers of T-RFs and T-RF-based Shannon diversity. For sample name,

648 upper case letters refer to treatment while digits indicate sampling time.

Sample	DNA		RNA	
	T-RFs	Shannon	T-RFs	Shannon
A1	11	1.55	23	2.55
B1	11	1.55	23	2.23
C1	11	1.49	22	2.17
D1	11	1.27	14	1.70
E1	11	1.48	20	2.12
F1	12	1.66	25	2.55
A7	12	1.74	28	2.92
B7	12	1.80	32	3.09
C7	13	1.77	27	2.86
D7	12	1.79	18	2.46
E7	14	1.89	30	2.98
F7	13	1.70	24	2.70
A14	13	1.70	36	3.17
B14	12	1.79	38	3.09
C14	12	1.83	33	2.96
D14	12	1.87	34	3.08
E14	12	1.83	32	2.89
F14	12	1.79	20	2.18

649

650

651

652

653

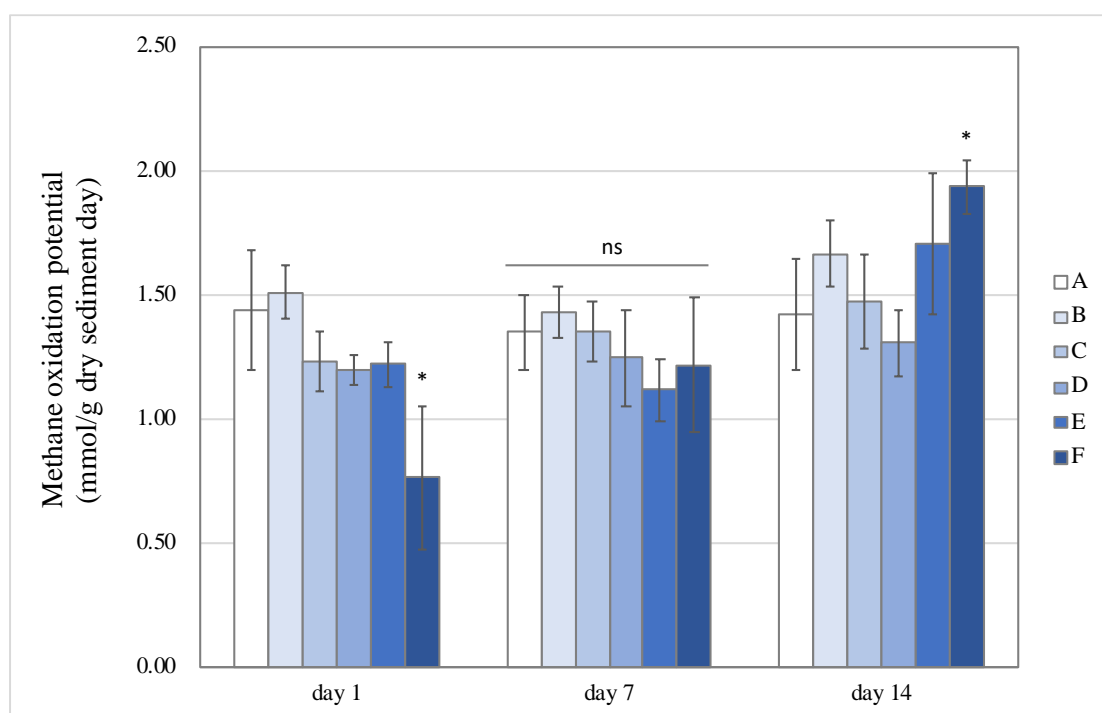
654

655

656

657 **Fig. 1.** Change of methane oxidation potential in the microcosms with different
658 treatments. Error bar indicates standard deviation ($n=3$). Asterisk indicates the
659 significance between experiment group and control group ($P < 0.05$). 'ns' indicates no
660 significant difference among treatments at a given time.

661



662

663

664

665

666

667

668

669

670

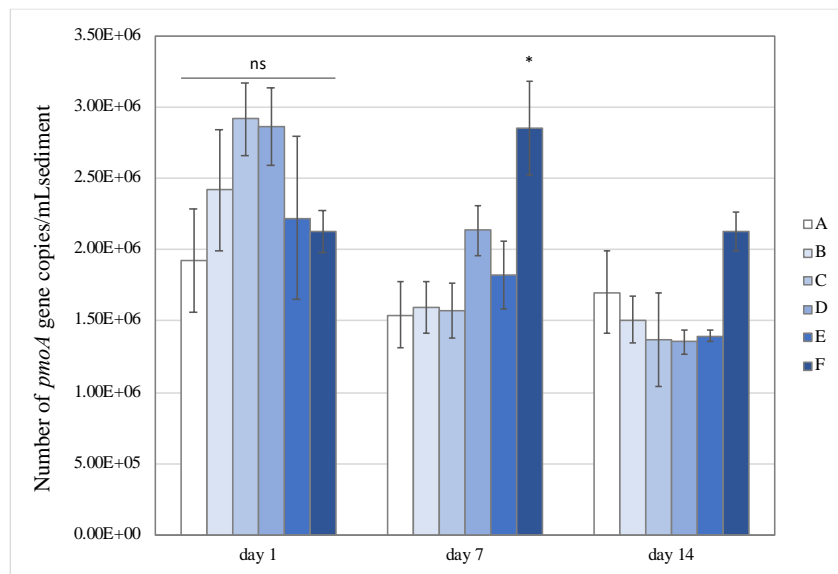
671

672

673

674 **Fig. 2.** Changes of *pmoA* gene (a) and transcript (b) abundance in the microcosms
 675 with different treatments. Error bar indicates standard deviation ($n=3$). Asterisk
 676 indicates the significance between experiment group and control group ($P < 0.05$). 'ns'
 677 indicates no significant difference among treatments at a given time.

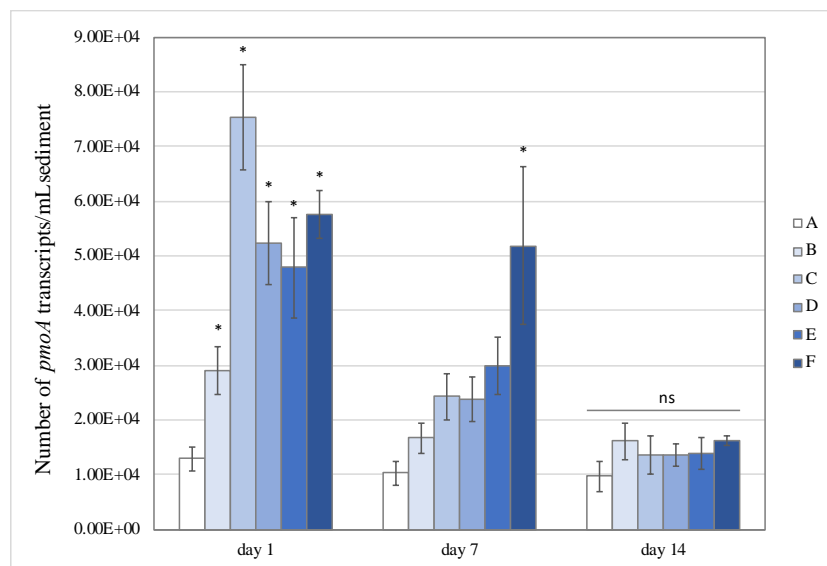
678 **(a)**



679

680

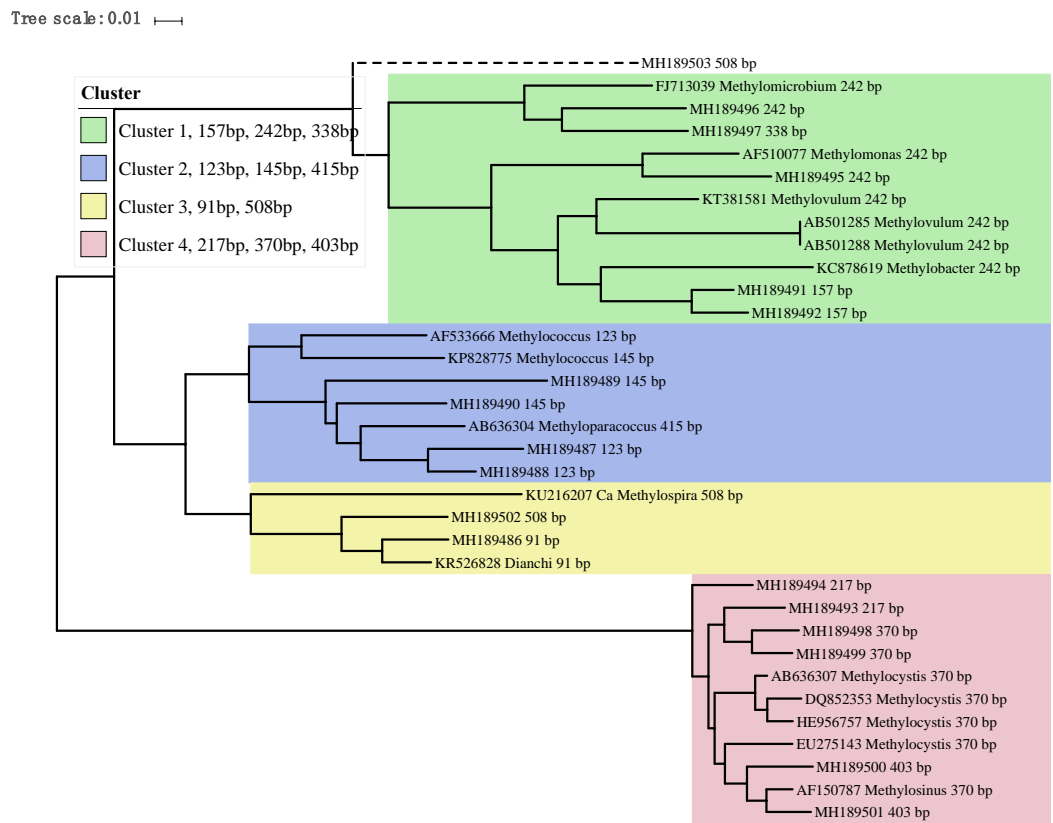
681 **(b)**



682

683

684 **Fig. 3.** Phylogenetic tree of obtained *pmoA* sequences and reference sequences from
 685 the GenBank database. The predicted cut sites were shown after the accession
 686 numbers of sequences. The dots at branches represent the support values from
 687 bootstrap test. Branch support values of no less than 50 were dotted. The bar
 688 represents 1% sequence divergence based on neighbor-joining algorithm.
 689



690
 691
 692
 693
 694
 695
 696
 697
 698

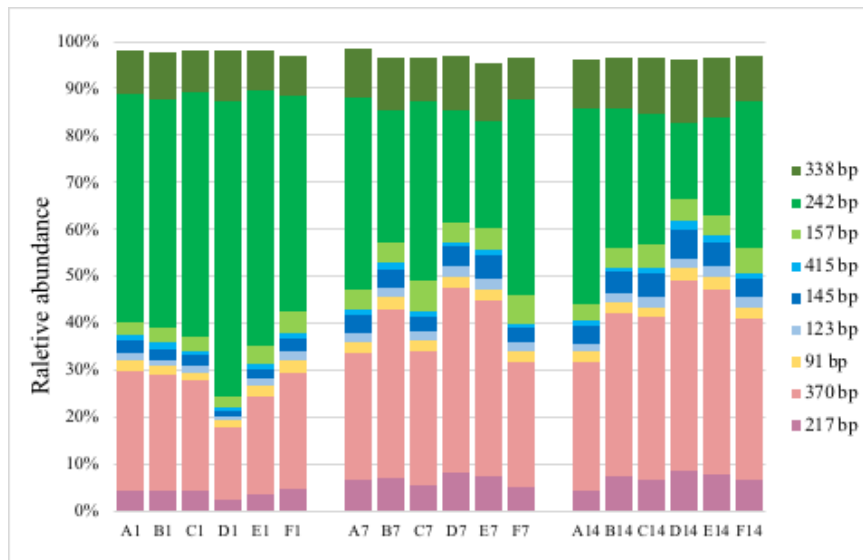
699

700

701 **Fig. 4.** T-RFLP profiles based on *pmoA* gene (a) and transcripts (b). For sample name,

702 upper case letters refer to treatment while digits indicate sampling time.

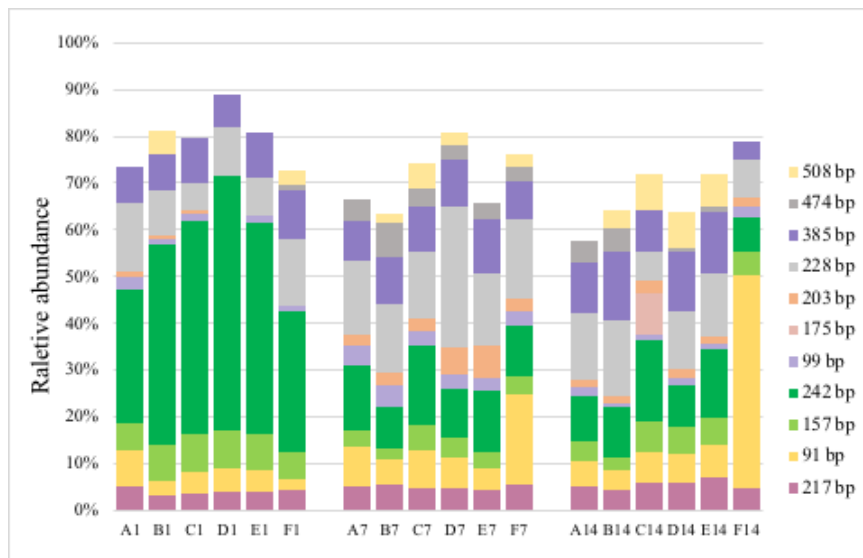
703 **(a)**



704

705

706 **(b)**



707

708

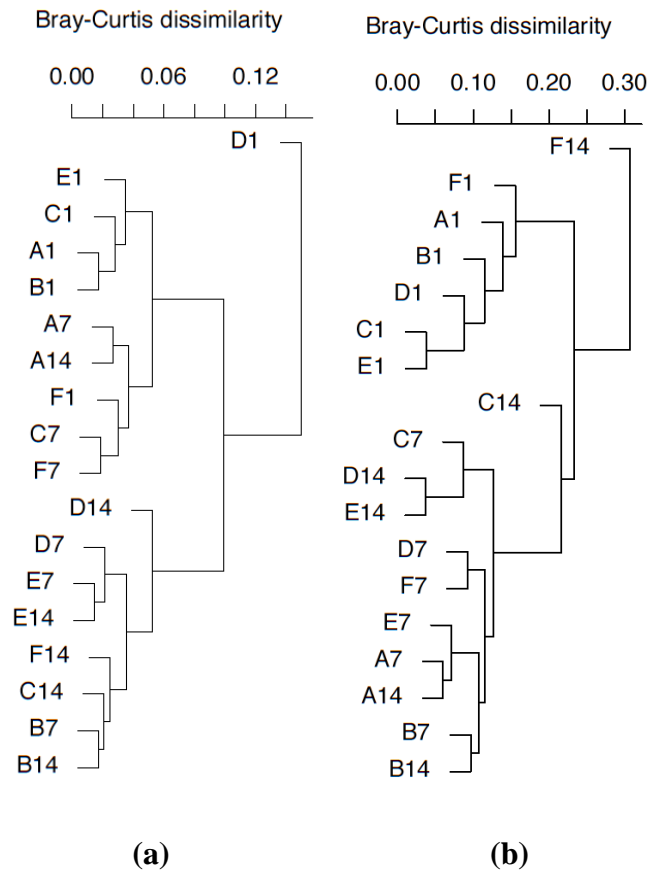
709

710

711

712

713 **Fig. 5.** *pmoA* gene (a) and transcripts (b)-based cluster diagrams of similarity values
714 for samples with different treatments. Dissimilarity levels are indicated above the
715 diagram. For sample name, upper case letters refer to treatment while digits indicate
716 sampling time.
717



718

719

720

721

722

723

724

725

726

727

728

Supplementary Material

729 **Table S1** Multiple comparison of treatments by means of Student-Newman-Keuls
730 post-hoc testing. In each column, different characters indicate significant difference at
731 0.05 level.

732

treatment	MOP		<i>pmoA</i> abundance		transcript abundance	
	Day 1	Day 14	Day 7	Day 14	Day 1	Day 7
A	a	b	b	ab	d	b
B	a	ab	b	b	c	b
C	a	b	b	b	a	b
D	a	b	b	b	b	b
E	a	ab	b	b	b	b
F	b	a	a	a	b	a

733

734

735

736

737

738

739

740

741

742

743

744

745

746

747

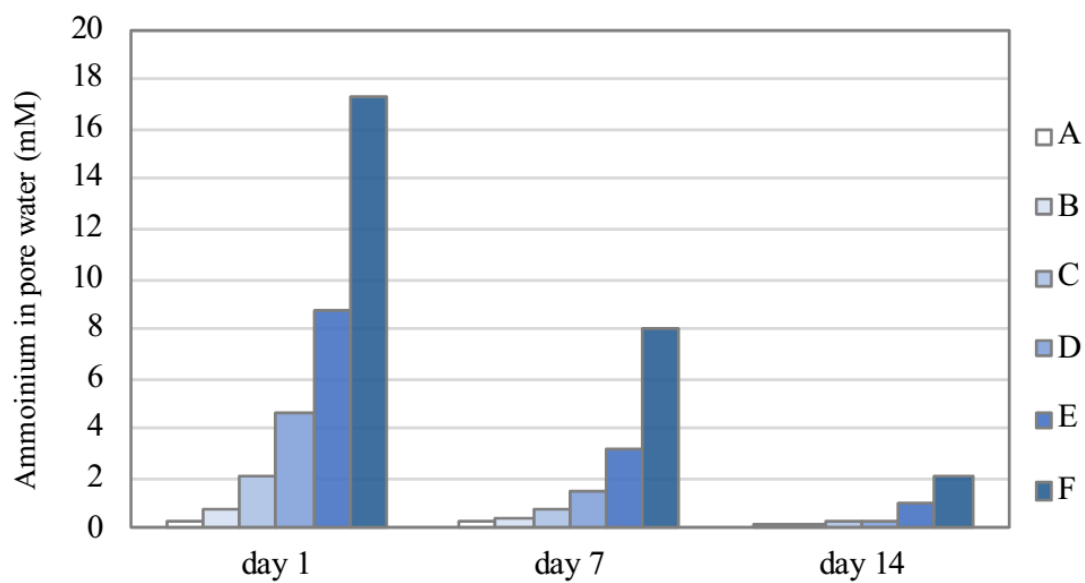
748

749

750 **Fig. S1.** Change of ammonium concentration of pore water in the microcosms with

751 different treatments

752



753

754

755

756

757

758

759

760

761

762

763

764

765

766

767

768

769

770

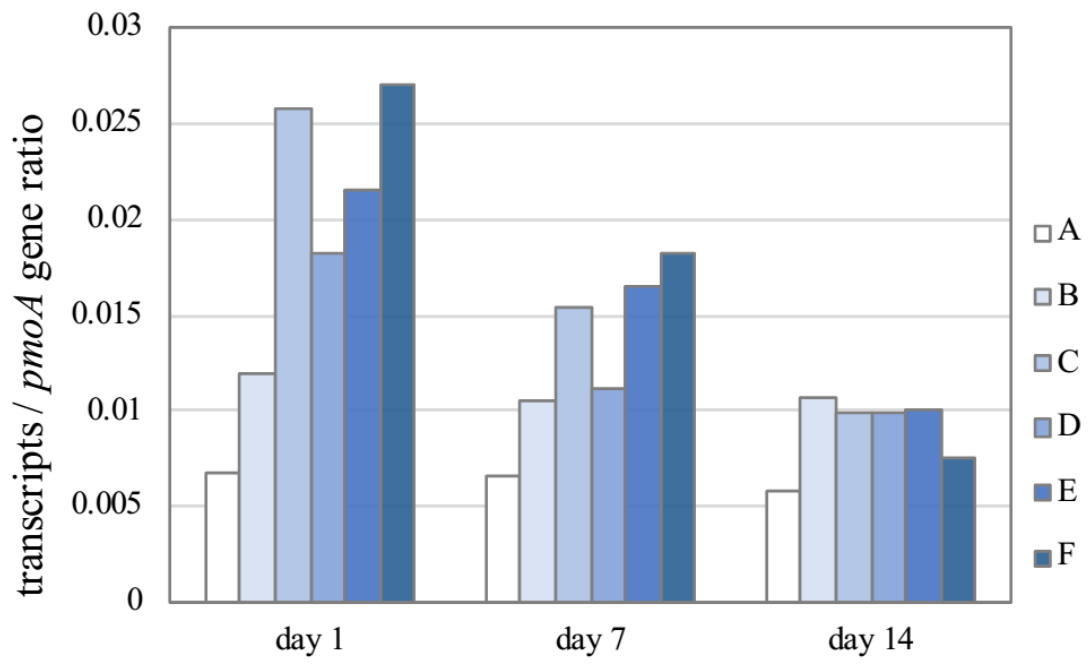
771

772

773
774
775

776 **Fig. S2.** The ratio of transcripts to *pmoA* gene in the microcosms with different
777 treatments

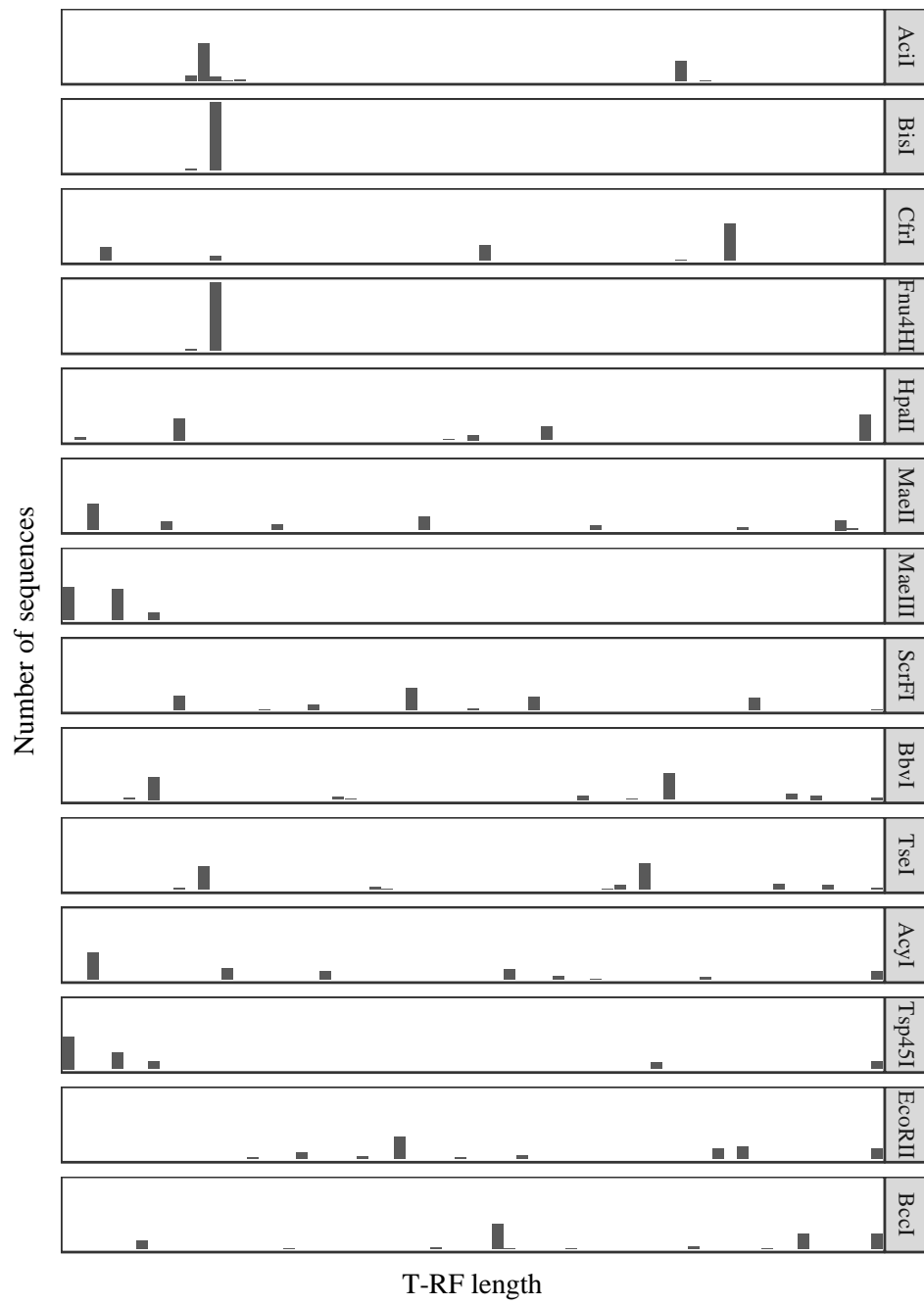
778



779
780
781
782
783
784
785
786
787
788
789
790
791
792
793
794
795
796

797
798
799
800

801 **Fig. S3.** Prediction of NGS representative sequences based on T-RFs



802
803
804